

## Original Article

# Activated autophagy contributes to the development of lymphatic malformations

Wen-Qun Zhong<sup>1</sup>, Wei Zhang<sup>1,2</sup>, Lu Gao<sup>1</sup>, Gang Chen<sup>1,2</sup>, Guo-Liang Sa<sup>1</sup>, Jie-Gang Yang<sup>1</sup>, Yi-Fang Zhao<sup>1,2</sup>, Yan-Fang Sun<sup>1,2</sup>

<sup>1</sup>The State Key Laboratory Breeding Base of Basic Science of Stomatology (Hubei-MOST) & Key Laboratory of Oral Biomedicine Ministry of Education, Wuhan University, Wuhan, China; <sup>2</sup>Department of Oral and Maxillofacial Surgery, School & Hospital of Stomatology, Wuhan University, Wuhan, China

Received February 10, 2017; Accepted March 20, 2017; Epub May 1, 2017; Published May 15, 2017

**Abstract:** To investigate the level of autophagy in lymphatic malformations (LMs), and the role of autophagy in the development of LMs, immunohistochemistry was used to examine the expression level of autophagy-related proteins [Beclin-1, Sequestosome 1 p62 (p62), light chain 3 (LC3)], and markers of anti-apoptosis [B cell lymphoma 2 (Bcl-2), phosphorylated extracellular signal-regulated kinase 1/2 (p-Erk1/2)] as well as the marker of proliferation (Ki-67) in samples of LMs and normal skins (SKs). The Pearson's correlation and cluster analyses were performed to determine to relationships between the proteins we tested. The studies using human dermal lymphatic endothelial cells (HDLECs) were carried out for mechanism investigation. Besides, rat models of LMs were established to evaluate the role of autophagy in LMs. The results showed that the autophagy-related proteins we tested, correlated with each other, were significantly increased in LMs compared with SKs samples. In vitro, autophagy, depended on p-Erk1/2, prevented the apoptosis of HDLECs in FBS starvation conditions. Furthermore, the correlation between the autophagy-related proteins, and p-Erk1/2 as well as Bcl-2 in LMs samples was confirmed in LMs samples. In the LM rat model, the inhibition of autophagy suppressed the development of LMs. Our study indicates that autophagy is elevated in LMs, and plays an important role in LMs.

**Keywords:** Lymphatic malformations, autophagy, anti-apoptosis, proliferation

## Introduction

Lymphatic malformations (LMs) are congenital anomalies related to the dysregulated lymphangiogenesis of the lymphatic system [1]. Compared to the trunk and extremities, the head and neck region is the major site for lymphatic malformations [2]. Due to their location, they cannot only cause aesthetic and development deformities, but also compromise the airway leading to breath problem, which could threaten the patients' life [3]. Up to date, management strategies for LMs include surgical resection, sclerotherapy, simple observation, laser, radiofrequency ablation, photodynamic therapy and intralesional endoscopy. Nevertheless, the treatment efficacy for LMs is still unclear as the mechanism behind the pathogenesis of this disease is largely unknown [4].

LMs are composed of abnormal dilated lymphatic channels lined with lymphatic endotheli-

al cells (LECs) [5]. In the embryo stage, lymphatic vessels develop from a subpopulation of Prox1<sup>+</sup> endothelial cells which were derived from lymph sacs [6]. Recently, studies have indicated that the higher survival and proliferative potential in the lining LECs of LMs characterized by elevated activation of the PI3K/AKT/mTOR and MEK/ERK signaling pathways, both of which were important regulators of cell growth and survival [1, 5, 7]. However, the accurate mechanism remains to be investigated.

Autophagy, a lysosome-dependent, dynamic degradation process, has been confirmed to be functional in various physiological processes as well as pathogenesis of various diseases [8]. Generally, autophagy is mainly mediated by the formation of double-membrane or multimembrane vesicles which are called autophagosomes that turnover and recycle proteins and organelles. Afterwards, the autophagosomes fuse with the lysosomal vesicles to form autoly-

## Autophagy in lymphatic malformation

sosomes where the maturation process could be finally completed [9]. This biological process requires the expression of a series of key genes related to autophagy, including microtubule-associated protein 1 light chain (LC3) [10], Beclin-1 [11], and Sequestosome 1 (p62) [12]. Numerous studies including our previous studies have implicated that the main role of autophagy was to ensure cell growth and survival even under stress conditions [9, 13, 14]. However, to our best knowledge, the status of autophagy and its role in the pathogenesis of LMs, a congenital anomaly of the lymphatic system, are largely unreported.

Therefore, here, the activated status of autophagy in the tissue samples of LMs was, for the first time, evaluated. Meanwhile, we also investigated the relationship of autophagy with cellular anti-apoptosis and proliferation in LMs. Moreover, *in vitro* studies showed that autophagy, depended on the activation of ERK1/2 pathway, was essential for the survival of human dermal lymphatic endothelial cells (HLEDs) in serum starvation condition. More importantly, inhibition of autophagy in a rat model of LMs significantly suppressed the development of LMs.

### Materials and methods

#### *Samples, immunohistochemistry and double-labelling immunofluorescence*

This study was approved by the review board of the Ethics Committee of Hospital of Stomatology, Wuhan University. Twenty-six tissue samples of lymphatic malformations, and 10 clinical samples of normal skins resected during plastic surgery were obtained at Hospital of Stomatology, Wuhan University. Meanwhile, informed consent for this study was got from all the subjects. The basic information for the patients with LMs is shown in [Supplementary Table 1](#). These specimens were fixed in buffered 4% paraformaldehyde before embedded in paraffin. For immunohistochemical and double-labelling immunofluorescence, the procedures were described as our previous studies [15, 16], which were depended on the National Institutes of Health guidelines as to the use of human tissues. Meanwhile, primary antibodies used in our studies were listed in [Supplementary Table 2](#).

#### *Transmission electron microscopy, immunofluorescence for LC3 localization and detection of acidic vesicular organelles (AVO)*

Transmission electron microscopy, immunofluorescence for LC3 localization and detection of acidic vesicular organelles (AVO) were performed as our previous description [17, 18] in the [Supplementary](#).

#### *Real-time quantitative PCR, Western blot analysis and flow cytometric analyses*

According to our previous protocol [15-17], real-time quantitative PCR (qPCR), western blot (WB) and flow cytometric analyses were carried out, all of which was described in the [Supplementary](#). In addition, the primer nucleotide sequences for PCR are listed in [Supplementary Table 3](#).

#### *Animal model of LMs in rats*

All animal experiments were approved by the Institutional Animal Care and Use Committee, Center for Animal Experiment, Wuhan University. Depended on our previous studies [19, 20], fifteen adult Wistar female rats, weighing  $250 \pm 30$  g were purchased from the Hubei Research Center of Laboratory Animals (Wuhan, China). Rats were randomly assigned into three groups: (i) subcutaneous injection of 200  $\mu$ l PBS every other week; (ii) subcutaneous injection of 100  $\mu$ l FIA (Santa Cruz Biotechnology, USA) + 100  $\mu$ l PBS every other week; (iii) subcutaneous injection of 100  $\mu$ l FIA (Santa Cruz Biotechnology, USA) + 100  $\mu$ l PBS every other week, and intraperitoneal injection of chloroquine 60 mg/kg 3 times a week. LMs in rats were monitored for every other week. After 2 months, animals were euthanized, and the lesions were collected for further studies [21].

#### *Statistical analysis*

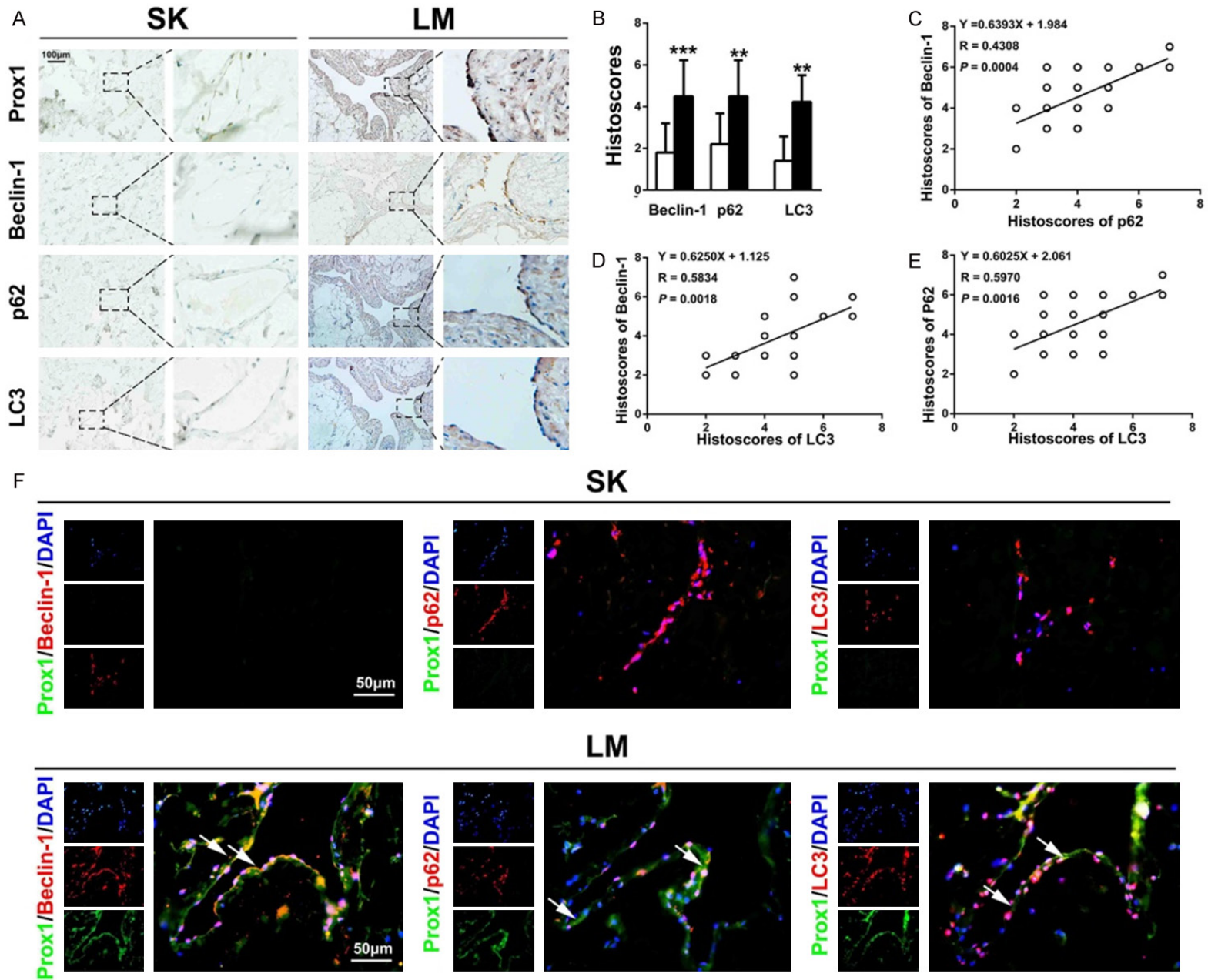
All data were represented as mean  $\pm$  SEM with three independent experiments. Statistical analysis was performed via Student's *t*-test, Spearman's rank correlation test and hierarchical clustering. Statistical significance was defined as  $P < 0.05$ .

### Results

#### *Activated autophagy in LMs*

To investigate the status of autophagy in LMs, the expression of some core autophagy-related

Autophagy in lymphatic malformation



## Autophagy in lymphatic malformation

**Figure 1.** Detection and evaluation of autophagy in lymphatic malformations (LMs). A. In the serial sections of the LM tissue samples, up-regulated expression of autophagy-related proteins (Beclin-1, p62 and LC3) in LMs compared with these in skin (SK) samples. B. Quantification of Beclin-1, p62 and LC3 expression levels in LM and SK samples. C-E. Spearman rank test showed a positive significant between these autophagy-related proteins. F. Double-labelling immunofluorescence staining for autophagy-related proteins (Beclin-1, p62 and LC3) and Prox1 in LM but SK samples. The white arrowheads indicated the colocalization of autophagy-related proteins with Prox1 signals. All data are presented as mean  $\pm$  SEM. **\*\*** $P < 0.01$  **\*\*\*** $P < 0.001$  versus control groups.

markers was detected and compared in 26 clinical samples of LMs and 10 of normal SKs by immunochemistry. As shown in **Figure 1A**, in the serial sections of tissue samples from LMs, we found that cytoplasmic staining for LC3, p62 and Beclin-1 in the Prox1<sup>+</sup> lymphatic endothelial cells (LECs), while the immunoreactivities for these proteins in SKs were much weaker. Importantly, the data from the Student's *t*-test for immunochemical staining showed that the expression levels of LC3 ( $P < 0.0001$ ), p62 ( $P < 0.0001$ ), and Beclin-1 ( $P < 0.01$ ) was significantly up-regulated in LMs than these proteins in SKs (**Figure 1B**). Furthermore, Spearman's rank correlation was performed and the results demonstrated that there was also a significant correlation between autophagy-related proteins (LC3, p62 or Beclin-1) (**Figure 1C-E**). Meanwhile, the double-labelling immunofluorescence analyses for Prox1 and Beclin-1, Prox1 and p62, Prox1 and LC3 were made on the samples both from the LMs and SKs, respectively, and we found that the colocalization of these proteins in LMs samples (**Figure 1F**). Collectively, these results strongly confirm the activation of autophagy in LMs.

### *Induction of autophagy with FBS-starvation*

To examine whether autophagy could also be merged in human lymphatic endothelial cells *in vitro*, we conducted the studies using HDLECs treated with normal FBS (20% FBS) or low FBS (5% FBS). As shown in **Figure 2A, 2B**, the data from TEM analysis showed that exposure of HDLECs to 5% FBS possessed more membranous vacuoles (AVs), resembling the autophagosomes when compared with the control groups. Meanwhile, we also observed autophagic response to low FBS via analysis of recruitment of punctate LC3, as well as appearance of yellow-orange AVOs, which were the hallmarks of autophagy. The data indicated that HDLECs in the control groups came up with weak and diffuse LC3 immunostaining, while the HDLECs in low FBS or rapamycin (positive

control) showed punctate pattern of LC3-associated green fluorescence. On the other hand, similar results could also be found in the formation of yellow-orange AVOs. In addition, the treatment of low FBS also resulted in elevated expression of autophagy-associated genes, including LC3, p62, Beclin-1, Atg2, Atg3, Atg5 and Atg7, in HDLECs, as well as autophagic proteins (Beclin-1 and LC3) (**Figure 2C, 2D**). Furthermore, to distinguish the autophagosome accumulation due to a block of downstream steps, we performed LC3 turnover assay via western blot analysis with Bafilomycin A1 (the lysosomal inhibitor) to measure the influence of low FBS on autophagic flux. The results exhibited that the difference in LC3-II levels with or without Bafilomycin A1 was much larger in low FBS when compared with the cells in normal condition, revealed that autophagic flux induced in HDLECs was indeed activated by low FBS (**Figure 2E**).

### *Inhibiting autophagy under low FBS enhanced apoptotic cell death*

To examine whether the suppression of autophagy could accelerate the cell death in low serum condition, chloroquine (CQ), a well-characterized inhibitor of autophagic flux, was carried out in combination with low serum starvation. As shown in **Figure 3A**, the results from flow cytometry showed that the population of Annexin V<sup>+</sup> apoptotic cells was markedly increased after treatment with CQ before serum starvation. Consistently, the DNA fragmentation assay was performed and the data indicated that incubation of CQ before serum starvation elicited obvious increase of DNA fragments in HDLECs (**Figure 3B**). Furthermore, the results from western blot analyses also demonstrated that the ratio of Bax/Bcl-2 as well as cleaved PARP in HDLECs were significantly up-regulated under the condition of incubation with CQ before serum starvation (**Figure 3C, 3D**). Thus, our results confirm that the apoptosis induced by low FBS could be enhanced by the inhibition of autophagy.

## Autophagy in lymphatic malformation

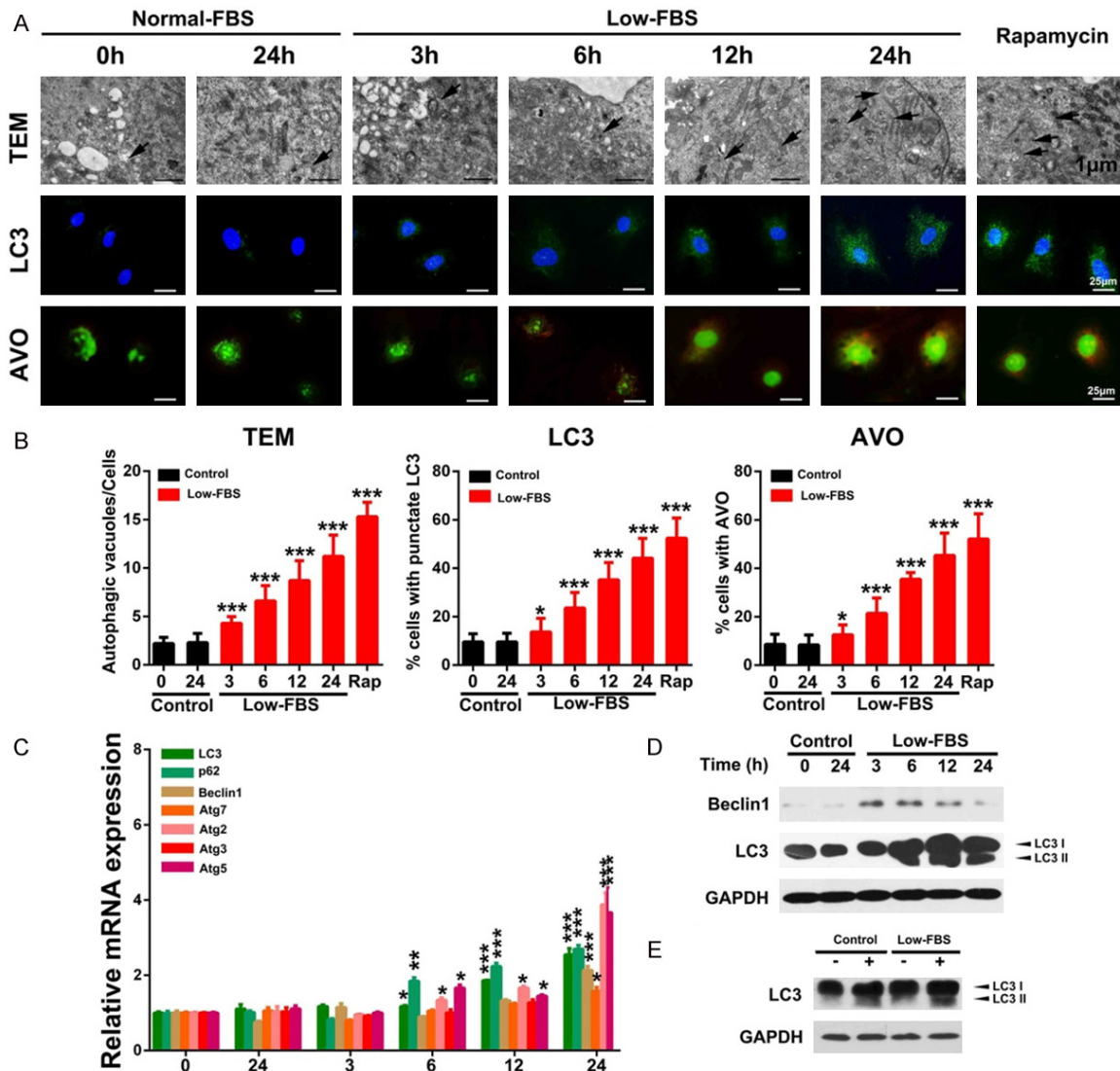


**Figure 2.** Low FBS causes autophagy in human dermal lymphatic endothelial cells (HDLECs). A. Detection for low FBS-induced autophagosomes by transmission electron microscopy (TEM), immunofluorescence (IF) and formation of yellow-orange AVO (AVO). B. Quantification of autophagosomes in HDLECs with TEM, IF and AVO. C. The effect of low FBS on the expression levels of autophagy-related genes was investigated by the real-time quantitative PCR. D. The expression status of Beclin-1 and LC3 were detected by western blotting (WB). E. The difference in the expression levels of LC3 between samples with and without Bafilomycin A1 was compared under normal and low FBS conditions by WB. All data are presented as mean  $\pm$  SEM. \* $P < 0.05$ , \*\* $P < 0.01$  \*\*\* $P < 0.001$  versus control groups.

### *Serum starvation activated autophagy via the Erk1/2 signaling pathway*

Recently, the Erk1/2 signaling pathway was proved to be pivotal in the activation of autophagy [10]. Thus, we tried to investigate whether Erk1/2 could be the upstream mediators for low serum-induced autophagy. As shown in **Figure 4**, low serum led to a rise in the expression level of Erk1/2 phosphorylation (p-Erk1/2) with a significant difference

at 3 h post treatment. Meanwhile, low FBS-induced p-Erk1/2 was greatly inhibited when HDLECs were pretreated with PD98059, a specific small-molecule inhibitor for p-Erk1/2 (**Figure 4A, 4B**). To our interests, PD98059 also significantly down-regulated the expression levels of Beclin-1 and the LC3II/LC3I ratio (**Figure 4C-F**). These results reveal that the activation of autophagy in HDLECs is depended on the activation of Erk1/2 signaling pathway under FBS starvation.

## Autophagy in lymphatic malformation

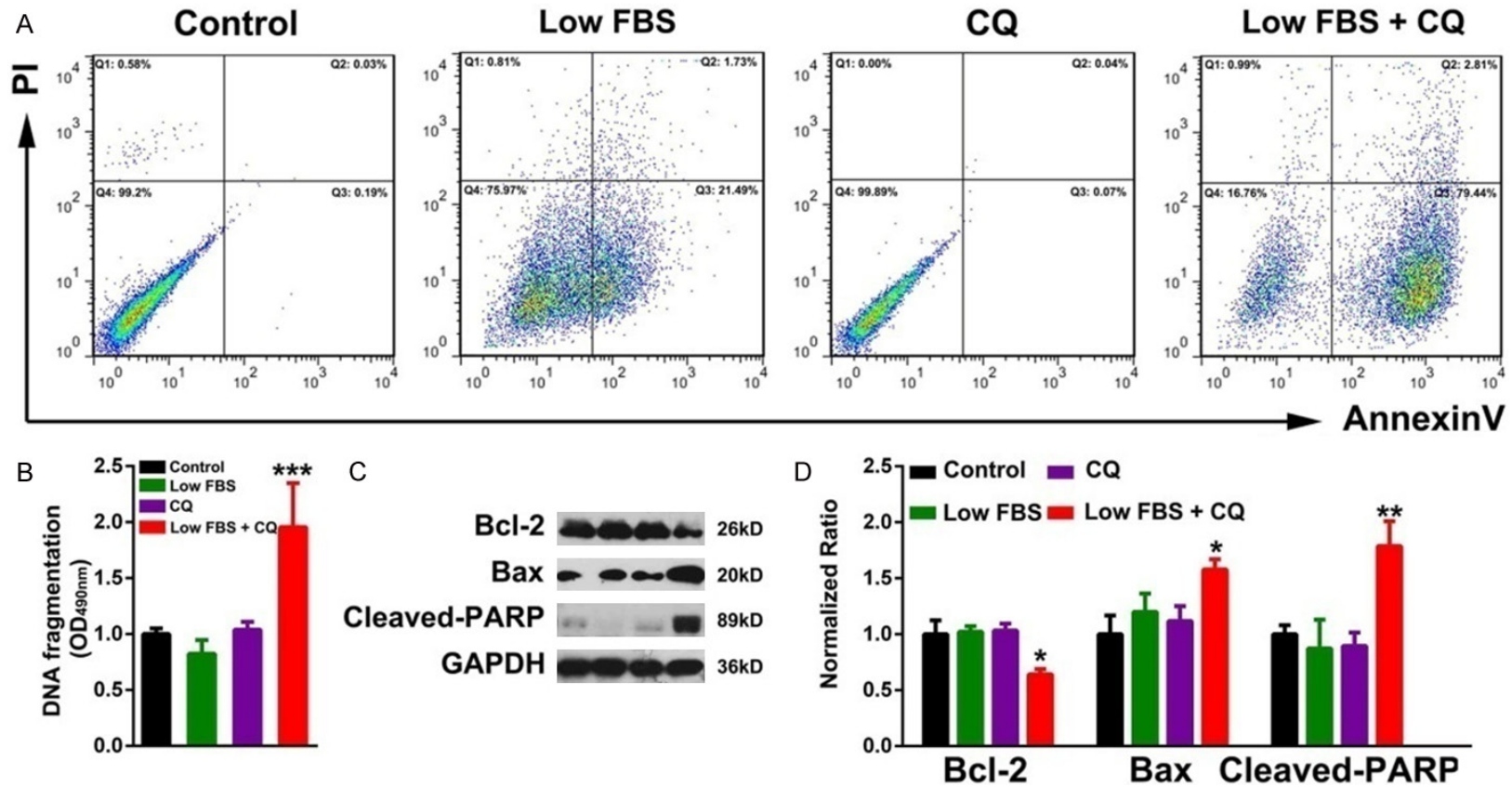


**Figure 3.** Low FBS-induced apoptosis is enhanced by inhibiting autophagy. A. HDLECs pre-treated with or without chloroquine (CQ) were cultured in low FBS condition for 24 h, and apoptosis rate was detected by Annexin V-FITC/PI dual labelling using flow cytometry. B. An augmentation of DNA fragmentation of low FBS-treated HDLECs was found after CQ pre-treatment. C. The expression levels of apoptosis-related proteins were determined by using western blot analysis. D. Relative quantitative data for apoptosis-related proteins were calculated by Image J. \* $P < 0.05$ , \*\* $P < 0.01$  versus control groups.

## Autophagy in lymphatic malformation

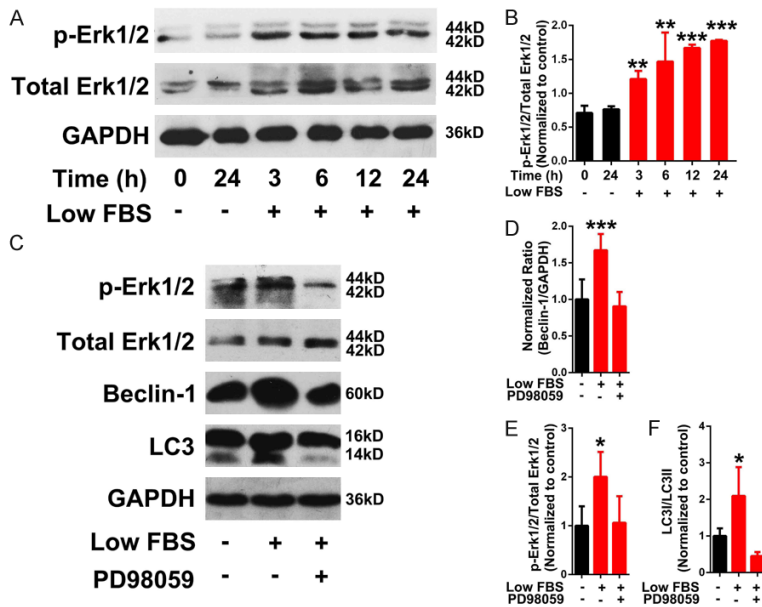


**Figure 4.** Low FBS-induced autophagy involves the ERK pathways in HDLECs. A. HDLECs exposed to low FBS for 3, 6, 12 and 24 h and showed an increase in Erk1/2 phosphorylation compared with those in normal FBS condition. B. Densitometric analysis of p-Erk1/2 level to total Erk1/2 level by using Image J. C. Expression levels of Beclin-1 and the ratio of p-Erk to total p-Erk, LC3I to LC3II, were down-regulated at 24 h using the p-Erk inhibitor (PD98059). D-F. Quantification of protein levels with the PD98059 treatment showed that the expression level of Beclin-1, and the ratio of p-Erk1/2 to total p-Erk1/2, LC3I to LC3II, were significantly down-regulated in 24 h. \* $P < 0.05$ , \*\* $P < 0.01$ , \*\*\* $P < 0.001$  versus control groups.

### Significant correlation between autophagy-related proteins and p-Erk1/2, Bcl-2 and Ki-67 in LMs clinical samples

To further explore the role of autophagy in the cellular anti-apoptosis and proliferation of LMs. We detected the expression of p-Erk1/2, Bcl-2, and Ki-67 in LMs samples via immunohistochemistry. The representative images are shown in **Figure 5A**. We found that the expression levels of p-Erk1/2, Bcl-2 and Ki-67 in LECs were significantly increased in lymphatic vessels of LMs when compared with these proteins in SKs (**Figure 5A, 5B**). Furthermore, Spearman's rank correlation revealed that there was closely positive correlation between LC3 and Bcl-2 or Ki-67, p62 and Ki-67, p-Erk1/2 and LC3, Bcl-2 or Ki-67 (**Figure 5C-H**). Moreover, clustering analysis for these tested markers was conducted, which was visualized with a heat map (**Figure 5I**). As shown in the heat map, almost all the LMs samples clustered together, which was obviously distinct from the cluster of SKs samples. Besides, this clustering

indicated that the expression of autophagy-related markers, was closely associated with the expression of Bcl-2, p-Erk1/2 and Ki-67, implicating internal relations between these proteins we tested.

### Suppression of autophagy inhibited the development of IFA-induced LMs

Previous researches including our studies showed that Freund's incomplete adjuvant (FIA) could be used to induce LMs in rats [19, 22] but the mechanism behind is unclear. To ascertain whether or not targeting autophagy in LMs can block or delay the development of LMs, we performed a chemopreventive treatment on IFA-induced LMs with chloroquine (CQ). As shown in **Figure 6A, 6B**, CQ significantly prevented the growth of FIA-induced LMs. On the other hand, the systemic toxicity was also preliminarily assessed. None of weight loss

(**Figure 6C**), ulceration in the skin, toxic response and death was found. Moreover, the H&E stained sections of heart, liver, spleen, lung and kidney showed no organ hemorrhage or other significant histopathological lesions could be found in the organs with the treatment of FIA and CQ (**Supplementary Figure 1**). Furthermore, by performing immunohistochemistry, we found that the expression of Ki-67, Bcl-2 as well as VEGF-C in LMs treated with CQ was largely reduced when compared with the control groups in **Figure 6D** and **Supplementary Figure 2**). All of the above results indicate that inhibiting autophagy with CQ could effectively suppress the development of IFA-induced LMs with high systematic biocompatibility.

### Discussion

Here, we demonstrated the autophagy process in LMs for the first time, and implicated that it might contribute to the anti-apoptosis and proliferation of lymphatic endothelial cells in LMs. Moreover, we also showed autophagic activa-



## Autophagy in lymphatic malformation

expression levels of LC3 showed significant positive correlation with Bcl-2. D. The expression levels of LC3 showed significant positive correlation with Ki-67. E. The expression levels of p62 showed significant positive correlation with Ki-67. F. The expression levels of p-Erk1/2 showed significant positive correlation with LC3. G. The expression levels of p-Erk1/2 showed significant positive correlation with Bcl-2. H. The expression levels of p-Erk1/2 showed significant positive correlation with Ki-67. I. Hierarchical clustering analyses for immunohistochemical staining of p62, LC3, Beclin-1, Bcl-2, p-Erk1/2, Ki-67 and VEGF-C in human LM samples. \*\*\* $P < 0.001$  versus control groups.

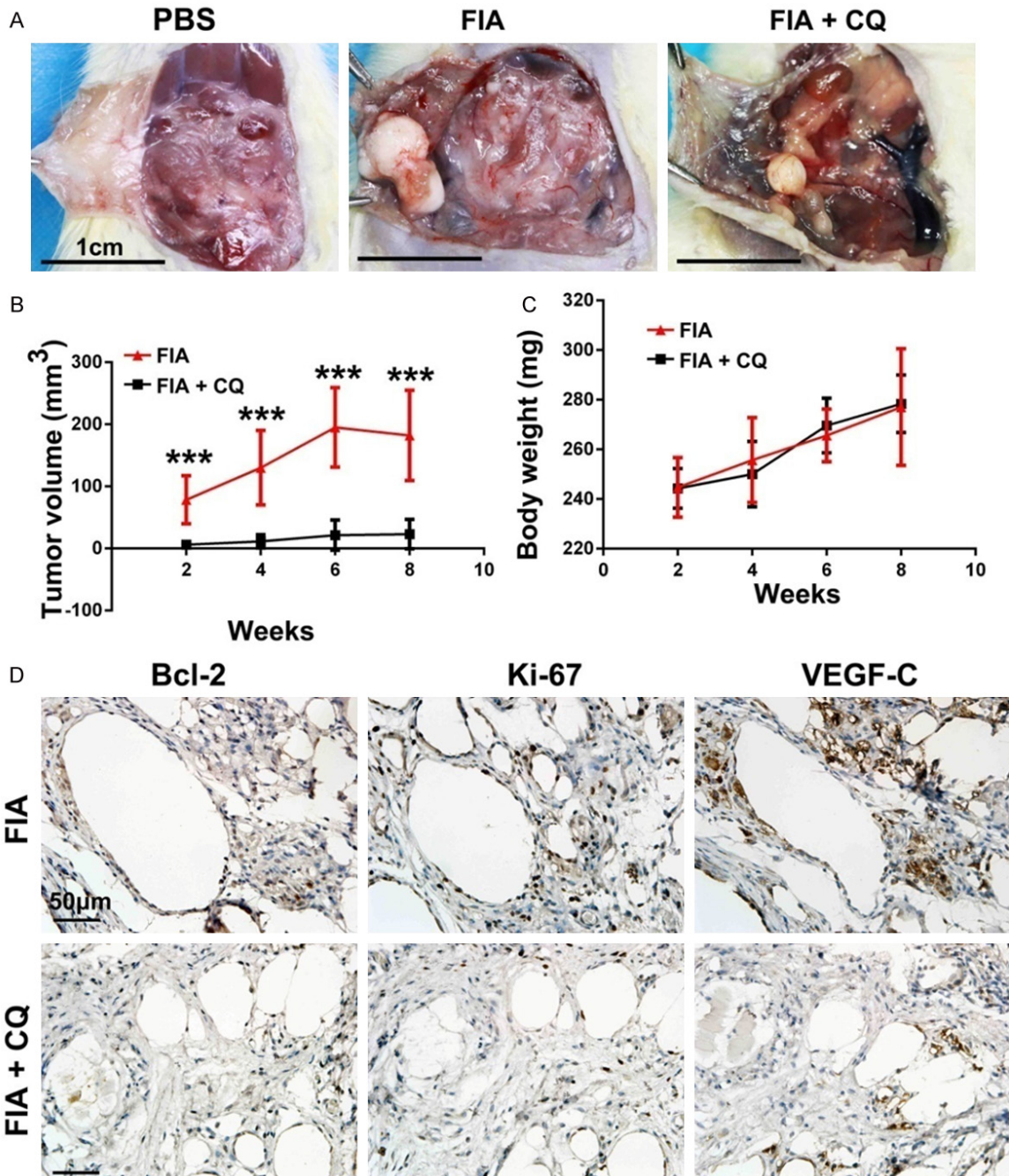


**Figure 6.** Suppression of autophagy prevented the anti-apoptosis and growth of IFA-induced LMs in rats. A. LMs regression was observed in IFA-induced LMs in rats treated with CQ. B. The size of IFA-induced LMs of rats in both CQ- and vehicle-treated groups was assessed every other week. C. Body weight of rats was measured every other week and showed that no side effect of CQ treatment. D. Immunohistochemical staining of the indicated biomarkers in IFA-induced LMs of rats treated with or without CQ treatment, which showed that decreased expression of Bcl-2, Ki-67 and VEGF-C was observed in FIA-induced LMs of rats treated with CQ when compared with the control groups.

## Autophagy in lymphatic malformation

tion in lymphatic endothelial cells (HDLECs), with the activation of ERK1/2 signal pathway in low FBS condition. In addition, our *in vivo* study also revealed that autophagy could be a promising target for the treatment of FIA induced-LMs in rats.

To date, more than 30 autophagic proteins have been recognized during autophagy-related processes [9, 13]. Among them, LC3, generally used to monitor the status of autophagy, is documented as the first mammalian protein bounded with autophagic membranes [8, 9]. p62 is selectively merged into autophagosomes by directly bonding with LC3 [9]. Besides, Beclin-1 is essential for vacuolar transport during autophagic processes [11]. Our study showed that these autophagic proteins, correlated with each other, were significantly increased, indicating an activated statue of autophagy in LMs.

Autophagy is a conserved catabolic process where damaged organelles, bacteria and misfolded proteins are transported into lysosomes for degradation [9, 10]. Numerous studies have confirmed that the primary role of autophagy was to ensure cellular survival under stress condition [8, 9, 14]. However, it is still vague that autophagy could be activated and its accurate role in lymphatic endothelial cells. Thus, *in vitro* studies using HDLECs were performed. As expected, autophagic activation could be observed in HDLECs, which was confirmed by our date from TEM, immunofluorescent, AVO staining, qPCR and western blot. Moreover, the date from flow cytometry, DNA fragments detection and western blot showed an increased apoptosis after inhibiting autophagy with CQ, a widely used autophagic pathway inhibitor [23], which indicated a pro-survival role of autophagy in HDLECs in low FBS condition. Therefore, based on the above results, we can draw a conclusion that autophagy could be activated in HDLECs and may contribute to the survival of these endothelial cells.

According to previous studies [14], there are two pathways well known to regulate autophagic response to nutrition starvation in mammalian cells: the class I phosphatidylinositol 3-phosphate kinase (PI3K)/Akt/mammalian target of rapamycin (mTOR)/p70 ribosomal protein S6 kinase (p70S6K) signaling pathway, and the Ras/Raf-1/mitogen-activated protein

kinase 1/2 (MEK1/2)/extracellular signal-regulated kinase 1/2 (Erk1/2) pathway. Among these, the Erk1/2 signal pathway positively regulates autophagy [24]. Correspondingly, our studies show that inhibition of the Erk1/2 signal pathway by a MAPK kinase (MAPKK) MEK1/2 inhibitor (PD98059) could inhibit FBS starvation-induced autophagy. Our date clearly showed that FBS-starvation up-regulated the Erk1/2 signaling pathway, leading to the activation of autophagy in HDLECs. More importantly, we found that in LMs samples, there were close correlations between autophagy core marker (LC3) and p-Erk1/2, Bcl-2 or Ki-67, which were confirmed by Spearman rank correlation test and the clustering analysis. Collectively, our results strongly suggested that autophagy may promote the anti-apoptosis and proliferation of lymphatic endothelial cells through the activation of Erk1/2 signaling pathway in LMs.

For clinical significance, we also used CQ to suppress the growth of IFA-induced LMs. Interestingly, the sizes of the IFA-induced LMs in rats were largely decreased after the treatment with CQ, followed by the weaken capacity of anti-apoptosis, proliferation and pro-lymphangiogenesis in lymphatic endothelial cells. Although further studies are needed to elucidate the mechanism, these findings suggest that defect of autophagy could restraint the development of IFA-induced LMs.

Here, our present study reported the activated status of autophagy in LMs and, simultaneously examined the underlying mechanism and pro-survival role of autophagy in the pathological processes of LMs. Our results also implicated that inhibition of autophagy could significantly suppress the development of LMs, revealing a new therapeutic strategy for LMs. Nevertheless, deeper investigation is still need to uncover the precise molecular mechanism in order to understand the pathogenic effect of autophagy for LMs.

### Acknowledgements

This study was supported by the National Natural Science Foundation of China (81371159, 81570994, 81500379), the specialized Research Fund for the Doctoral Program of Higher Education (20130141130006).

## Disclosure of conflict of interest

None.

**Address correspondence to:** Yi-Fang Zhao and Yan-Fang Sun, The State Key Laboratory Breeding Base of Basic Science of Stomatology (Hubei-MOST) & Key Laboratory of Oral Biomedicine Ministry of Education, School & Hospital of Stomatology, Wuhan University, 237 Luoyu Road, Wuhan 430079, China. E-mail: yifang@whu.edu.cn (YFZ); sunyanfang@whu.edu.cn (YFS)

## References

- [1] Brouillard P, Boon L and Vikkula M. Genetics of lymphatic anomalies. *J Clin Invest* 2014; 124: 898-904.
- [2] Hamoir M, Plouin-Gaudon I, Rombaux P, Francois G, Cornu AS, Desuter G, Clapuyt P, Debauche C, Verellen G and Beguin C. Lymphatic malformations of the head and neck: a retrospective review and a support for staging. *Head Neck* 2001; 23: 326-337.
- [3] Narkio-Makela M, Makela T, Saarinen P, Salminen P, Julkunen I and Pitkaranta A. Treatment of lymphatic malformations of head and neck with OK-432 sclerotherapy induce systemic inflammatory response. *Eur Arch Otorhinolaryngol* 2011; 268: 123-129.
- [4] Elluru RG, Balakrishnan K and Padua HM. Lymphatic malformations: diagnosis and management. *Semin Pediatr Surg* 2014; 23: 178-185.
- [5] Osborn AJ, Dickie P, Neilson DE, Glaser K, Lynch KA, Gupta A and Dickie BH. Activating PIK3CA alleles and lymphangiogenic phenotype of lymphatic endothelial cells isolated from lymphatic malformations. *Hum Mol Genet* 2015; 24: 926-938.
- [6] Wigle JT and Oliver G. Prox1 function is required for the development of the murine lymphatic system. *Cell* 1999; 98: 769-778.
- [7] Kurek KC, Luks VL, Ayturk UM, Alomari AI, Fishman SJ, Spencer SA, Mulliken JB, Bowen ME, Yamamoto GL, Kozakewich HP and Warman ML. Somatic mosaic activating mutations in PIK3CA cause CLOVES syndrome. *Am J Hum Genet* 2012; 90: 1108-1115.
- [8] Choi AM, Ryter SW and Levine B. Autophagy in human health and disease. *N Engl J Med* 2013; 368: 1845-1846.
- [9] Levine B and Kroemer G. Autophagy in the pathogenesis of disease. *Cell* 2008; 132: 27-42.
- [10] Martinez-Lopez N and Singh R. ATGs: scaffolds for MAPK/ERK signaling. *Autophagy* 2014; 10: 535-537.
- [11] Wirawan E, Lippens S, Vanden Berghe T, Romagnoli A, Fimia GM, Piacentini M and Vandenabeele P. Beclin1: a role in membrane dynamics and beyond. *Autophagy* 2012; 8: 6-17.
- [12] Johansen T and Lamark T. Selective autophagy mediated by autophagic adapter proteins. *Autophagy* 2011; 7: 279-296.
- [13] Li RF, Chen G, Zhao Y, Zhao YF and Liu B. Increased expression of autophagy-related proteins in keratocystic odontogenic tumours: its possible association with growth potential. *Br J Oral Maxillofac Surg* 2014; 52: 551-556.
- [14] Ma J, Wan J, Meng J, Banerjee S, Ramakrishnan S and Roy S. Methamphetamine induces autophagy as a pro-survival response against apoptotic endothelial cell death through the Kappa opioid receptor. *Cell Death Dis* 2014; 5: e1099.
- [15] Zhong WQ, Chen G, Zhang W, Xiong XP, Ren JG, Zhao Y, Liu B and Zhao YF. Down-regulation of connexin43 and connexin32 in keratocystic odontogenic tumours: potential association with clinical features. *Histopathology* 2015; 66: 798-807.
- [16] Zhong WQ, Chen G, Zhang W, Xiong XP, Zhao Y, Liu B and Zhao YF. M2-polarized macrophages in keratocystic odontogenic tumor: relation to tumor angiogenesis. *Sci Rep* 2015; 5: 15586.
- [17] Chen G, Zhang W, Li YP, Ren JG, Xu N, Liu H, Wang FQ, Sun ZJ, Jia J and Zhao YF. Hypoxia-induced autophagy in endothelial cells: a double-edged sword in the progression of infantile haemangioma? *Cardiovasc Res* 2013; 98: 437-448.
- [18] Zhao Y, Chen G, Zhang W, Xu N, Zhu JY, Jia J, Sun ZJ, Wang YN and Zhao YF. Autophagy regulates hypoxia-induced osteoclastogenesis through the HIF-1alpha/BNIP3 signaling pathway. *J Cell Physiol* 2012; 227: 639-648.
- [19] Sun Y, Jia J, Zhang W, Liu B, Zhang Z and Zhao Y. A reproducible in-vivo model of lymphatic malformation in rats. *J Comp Pathol* 2011; 145: 390-398.
- [20] Zhang W, He KF, Yang JG, Ren JG, Sun YF, Zhao JH and Zhao YF. Infiltration of M2-polarized macrophages in infected lymphatic malformations: possible role in disease progression. *Br J Dermatol* 2016; 175:102-112.
- [21] Ren JG, Wang HF, Chen G, Zhang W, Jia HZ, Feng J and Zhao YF. In vivo synergetic effect of in situ sclerotherapy and transient embolotherapy designed for fast-flow vascular malformation treatments with the aid of injectable hydrogel. *Journal of Materials Chemistry B* 2013; 1: 2601-2611.
- [22] Short RF, Shiels WE 2nd, Sferra TJ, Nicol KK, Schofield M and Wiet GJ. Site-specific induction of lymphatic malformations in a rat model

## Autophagy in lymphatic malformation

- for image-guided therapy. *Pediatr Radiol* 2007; 37: 530-534.
- [23] Rosenfeldt MT, O'Prey J, Morton JP, Nixon C, MacKay G, Mrowinska A, Au A, Rai TS, Zheng L, Ridgway R, Adams PD, Anderson KI, Gottlieb E, Sansom OJ and Ryan KM. p53 status determines the role of autophagy in pancreatic tumour development. *Nature* 2013; 504: 296-300.
- [24] Saiki S, Sasazawa Y, Imamichi Y, Kawajiri S, Fujimaki T, Tanida I, Kobayashi H, Sato F, Sato S, Ishikawa K, Imoto M and Hattori N. Caffeine induces apoptosis by enhancement of autophagy via PI3K/Akt/mTOR/p70S6K inhibition. *Autophagy* 2011; 7: 176-187.

## Autophagy in lymphatic malformation

**Supplementary Table 1.** Summary of clinical features of patients with lymphatic malformations

Patient	Sex	Age (years)	Location	Macro/microcystic
1	M	9	Tongue	Microcystic
2	M	15	Zygomatic area	Microcystic
3	F	2.5	Right cheek	Microcystic
4	M	25	Parotid region	Macrocytic
5	F	10	Tongue	Microcystic
6	M	9	Tongue	Microcystic
7	F	4	Upper lip	Microcystic
8	F	41	Tongue	Macrocytic
9	M	3	Tongue	Microcystic
10	M	11	Submandibular	Microcystic
11	M	3	Tongue	Microcystic
12	F	4	Upper lip	Microcystic
13	M	20	Right cheek	Microcystic
14	M	8	Tongue	Microcystic
15	M	18	Zygomatic area	Microcystic
16	M	16	Tongue	Microcystic
17	F	12	Tongue	Microcystic
18	M	4	Tongue	Microcystic
19	F	33	Parotid gland	Macrocytic
20	M	16	Tongue	Microcystic
21	M	13	Submandibular	Microcystic
22	M	18	Right cheek	Microcystic
23	M	8	Tongue	Microcystic
24	F	33	Tongue	Microcystic
25	M	13	Tongue	Microcystic
26	M	52	Tongue	Macrocytic

**Supplementary Table 2.** Summary of antibodies used in immunochemistry (IHC), immunofluorescence (IF-P) and western blot (WB)

Antibody	Source	Supplier	Dilution
Beclin-1	Goat mAb	SantaCruz (10086)	IHC (1:400)
			IF-P (1:200)
			WB (1:1000)
LC3	Rabbit mAb	Cell Signaling Technology (4108)	IHC (1:50)
			IF-P (1:25)
			WB (1:2000)
p62	Rabbit mAb	Abcam (ab109012)	IHC (1:200)
Bcl-2	Mouse mAb	Abcam (ab692)	IHC (1:200)
			IF-P (1:100)
			WB (1:1000)
Ki-67	Mouse mAb	SantaCruz (23900)	IHC (1:400)
			IF-P (1:100)
VEGF-C	Goat pAb	SantaCruz (27128)	IHC (1:400)
Bax	Rabbit mAb	Cell Signaling Technology (14796)	WB (1:1000)
		Cell Signaling Technology (5625)	
Cleaved PARP	Rabbit mAb	SantaCruz (365062)	WB (1:1000)
		Cell Signaling Technology (4695)	
GAPDH	Mouse mAb		WB (1:1000)
Total Erk1/2	Rabbit mAb		WB (1:1000)

## Supplementary information

### Supplementary materials and methods

#### *Cell culture and cell viability assay*

As our previous description [1], human dermal lymphatic endothelial cells (HDLECs) were obtained from Sciencell (Carlsbad, USA). HDLECs were cultured in endothelial cell medium (ECM; Sciencell, USA) with 20% fetal bovine serum (FBS), penicillin-streptomycin mixture and SingleQuot (Cambrex Bio Science). In our present study, cells in passages 2-7 were used. When the cells were grown to 70% confluence, they were cultured with low FBS (5% FBS) or normal FBS (20% FBS) for 24 h, respectively.

#### *Transmission electron microscopy*

As our previous description [2], For the transmission electron microscopy (TEM), HDLECs ( $2 \times 10^5$ ) were seeded into 6-cm dishes for overnight attachment, and then incubated with 10% FBS or 5% FBS for indicated time. Then, these HLECs were fixed by using 2.5% electron microscopy grade glutaraldehyde, and further postfixed in 1% osmium tetroxide with 0.1% potassium ferricyanide, followed by dehydrated through an orderly series of ethanol (30-90%). After embedded in Epon, ultrathin sections (65 nm) of cells were cut, routinely stained with 2% uranyl acetate as well as Reynold's lead citrate. Finally, these sections were observed using a transmission electron microscope (Hitachi H-600).

#### *Immunofluorescence for LC3 localization*

As we described previously [3, 4], HDLECs ( $2 \times 10^5$ ) were seeded to coverslips in 6-cm dishes and allowed to attach after overnight culture. After incubated with 5% FBS or 10% FBS for indicated time, these cells were fixed with 4% paraformaldehyde, and then permeabilized in 0.1% Triton X-100 for 20 min. Later, the cells were blocked with bovine serum albumin buffer for 1 h at 37 °C before incubated with the anti-LC3 antibody (1:50) overnight at 4 °C. Next, the cells were treated with fluorescein isothiocyanate (FITC)-conjugated donkey anti-rabbit second antibody (West Grove) for 1 h. Then, the cellular nuclei were stained with DAPI, observed and photographed under a fluorescence microscope (Leica).

#### *Detection of acidic vesicular organelles (AVO)*

According our previous procedures [2, 4], HDLECs ( $2 \times 10^5$ ) were plated on coverslips in 6-cm dishes. After attached on the coverslips, the cells were treated with 5% FBS or 10% FBS for definite time and then stained with 1 mg/ml acridine orange for 15 min. Immediately, these cells was photographed under a fluorescence microscope (Leica).

#### *Real-time quantitative PCR*

According to our previous protocol [5], real-time quantitative PCR (qPCR) was performed. Briefly, total RNA from HDLECs was isolated with TRIzol Reagent (Invitrogen). Afterwards, 2 µg RNA was reverse transcribed to cDNA with Oligo(dT) and AMV reverse transcriptase (Fermentas). Then, the cDNA was used for polymerase chain reaction (PCR) by using FastStart Universal SYBR Green Master (Roche) with a 7900HT Real-time PCR System (Applied Biosystems). In this assay, GAPDH was chosen to be the endogenous control, and the primer nucleotide sequences for PCR are presented in [Supplementary Table 3](#).

#### *Western blot analysis*

According to our previous protocol [2], the western blot was carried out. Briefly, HDLECs were lysed to the total protein which was then transferred onto polyvinylidene fluoride membranes (Millipore). Next, the blots were blocked in 5% non-fat dry milk for 1 h, followed by incubation with corresponding primary antibodies. After incubated with horseradish peroxidase-conjugated secondary antibody (Pierce Chemical), the blots were immersed in a SuperEnhanced chemiluminescence solution (Pierce, Rockford).

# Autophagy in lymphatic malformation

## *Flow cytometric analyses*

Depended on our previous studies [5], after culture in 5% FBS and 20% FBS with or without CQ,  $1 \times 10^6$  HDLECs were collected, stained with FITC-Annexin V and PE-PI for flow cytometry with BD fluorescent-activated cell sorter system (Calibur, CO) according to the manufacturer's instructions. Finally, the data was analyzed with FlowJo 7.6.1 software.

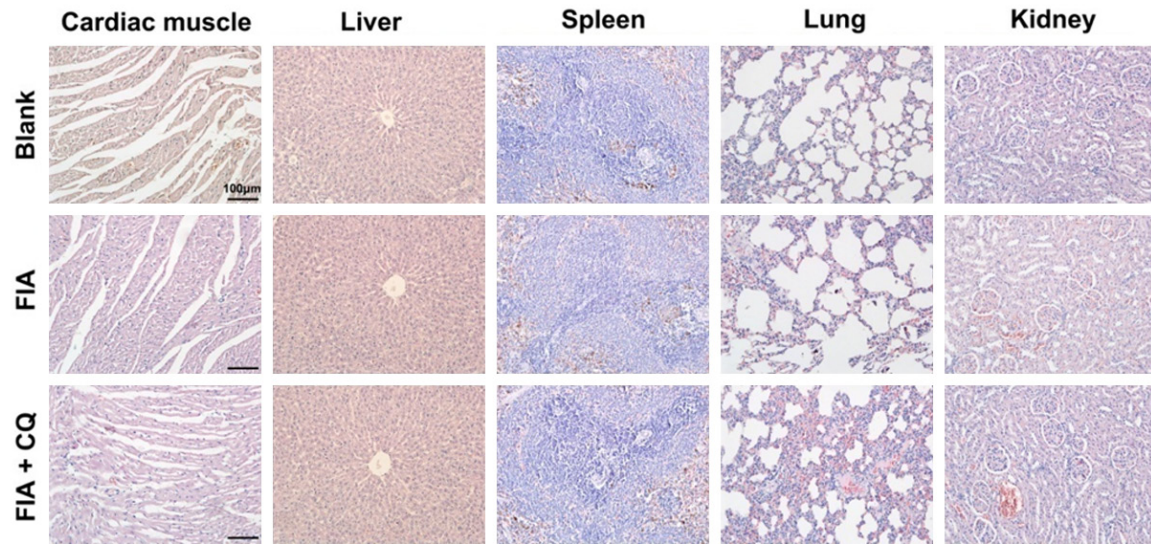
## **References**

- [1] Cai X, Zhang W, Chen G, Li RF, Sun YF and Zhao YF. Mesenchymal status of lymphatic endothelial cell: enlightening treatment of lymphatic malformation. *Int J Clin Exp Med* 2015; 8: 12239-12251.
- [2] Chen G, Zhang W, Li YP, Ren JG, Xu N, Liu H, Wang FQ, Sun ZJ, Jia J and Zhao YF. Hypoxia-induced autophagy in endothelial cells: a double-edged sword in the progression of infantile haemangioma? *Cardiovasc Res* 2013; 98: 437-448.
- [3] Levine B and Kroemer G. Autophagy in the pathogenesis of disease. *Cell* 2008; 132: 27-42.
- [4] Zhao Y, Chen G, Zhang W, Xu N, Zhu JY, Jia J, Sun ZJ, Wang YN and Zhao YF. Autophagy regulates hypoxia-induced osteoclastogenesis through the HIF-1 $\alpha$ /BNIP3 signaling pathway. *J Cell Physiol* 2012; 227: 639-648.
- [5] Zhong WQ, Chen G, Zhang W, Xiong XP, Zhao Y, Liu B and Zhao YF. M2-polarized macrophages in keratocystic odontogenic tumor: relation to tumor angiogenesis. *Sci Rep* 2015; 5: 15586.

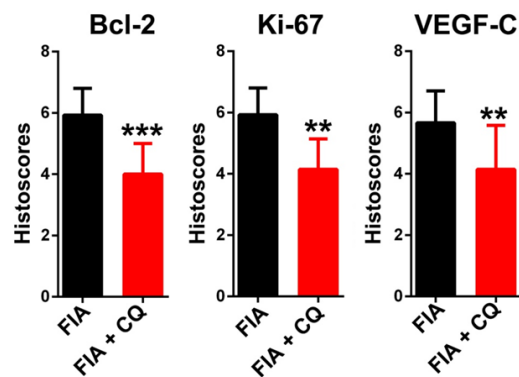
## Autophagy in lymphatic malformation

**Supplementary Table 3.** Primer sequences used for real-time quantitative PCR

Genes	Forward (5'-3')	Reverse (5'-3')
LC3	CGGAGCTTTGAACAAAGAGTG	TCTCTACTCTCGTACACTTC
p62	AGTGCCGTTATACTGTTCTG	ACTGCCTCCTGTGTCTTCAATCTT
Beclin-1	GCAAGCCCGCAGAGATGTGGA	GCAGCAATGACGGCAGGAAGC
Atg7	GCTGTGGAGCTGATGGTCTC	CCAGGCTGACAGGAAGAACA
Atg2	AGTACTAGTAAGGAGAGTGGAACCAGGAG	AGTAAGCTTCCTTTGCCAAAACTTTCA
Atg3	GACCCCGGTCCTCAAGGAA	TGTAGCCCATTGCCATGTTGG
Atg5	GCAAGCCAGACAGGAAAAAG	GACCTTCAGTTGGTCCGGTAA
GAPDH	CCATGTCGTCATGGGTGTAACCA	GCCAGTAGAGGCAGGGATGATGTTTC



**Supplementary Figure 1.** Photographs of hematoxylin-eosin staining for cardiac muscle, liver, spleen, lung and kidney organs of rats after the FIA treatment with or without CQ.



**Supplementary Figure 2.** Semi-quantification of immunohistochemical staining of Bcl-2, Ki-67 and VEGF-C in FIA-induced LMs of rats treated with or without chloroquine (CQ). \*\* $P < 0.01$  \*\*\* $P < 0.001$  versus control groups.